

## Theoretical Design and Advanced Microstructure in Super High Strength Steels

F. G. Caballero<sup>1</sup>, M. J. Santofimia<sup>2</sup>, C. García-Mateo<sup>1\*</sup>, J. Chao<sup>1</sup> and C. García de Andrés<sup>1</sup>

<sup>1</sup> Materialia Research Group, Department of Physical Metallurgy, Centro Nacional de Investigaciones Metalúrgicas (CENIM), Consejo Superior de Investigaciones Científicas (CSIC), Avda. Gregorio del Amo, 8. E-28040 Madrid, Spain

<sup>2</sup> Materials Innovation Institute (M2i), Department of Materials Science and Engineering, Delft University of Technology, Mekelweg 2, 2628 CD, Delft, The Netherlands

\* Corresponding author: Materialia Research Group, Department of Physical Metallurgy, Centro Nacional de Investigaciones Metalúrgicas (CENIM), Consejo Superior de Investigaciones Científicas (CSIC), Avda. Gregorio del Amo, 8. E-28040 Madrid, Spain. Tlf: 0034 91 553 89 00 (Ext 373); Fax 0034 91 534 7425; E-mail: [cgm@cenim.csic.es](mailto:cgm@cenim.csic.es)

## Abstract

A theoretical design procedure based on phase transformation theory alone has been successfully applied to design steels with a microstructure consisting of a mixture of bainitic ferrite and retained austenite. Using thermodynamics and kinetics models, a set of four carbide free bainitic steels with a 0.3 wt-% carbon content were designed and manufactured following a thermo-mechanical treatment consisting of hot rolling and two-step cooling. The designed steels present significant combinations of strength and ductility, with tensile strengths ranging from 1500 to 1800 MPa and total elongations over 15%. However, a carbon content of 0.3 wt% is still high for in-use properties such as weldability. In this sense, a reduction in the average carbon content of advanced bainitic steels was proposed. Improved bainitic steels with a carbon content of 0.2 wt% reached combinations of strength and ductility comparable to those in TRIP assisted steels.

**Keywords:** Ferrous metals and alloys; Microstructure; Mechanical Properties

## 1. Introduction

The demand for steel grades with increased strength levels and well balanced formability has strongly been increasing over the last years in applications fields such as automotive and truck. The main goal is the reduction of weight in vehicles, crane arms or any constructional element, thus a reduction of fuel consumption keeping or even improving safety standards. In this sense, apart from cold rolled high strength steel products also hot rolled steel grades for direct processing with high and super high strength levels have gained more and more a value added product.

New high-strength high-toughness carbide free bainitic steels have been recently designed using models based on phase transformation theory alone [1-3]. The designed steels, manufactured following conventional thermo-mechanical processes, reached significant combinations of strength and toughness, comparable to those of quenched and tempered martensitic steels.

The microstructure responsible of these mechanical properties consists of fine plates of bainitic ferrite separated by carbon-enriched regions of austenite. There may also be some martensite present. The advantages of obtaining this type of microstructure in flat products are also manifold. Because of the ultra fine grain size of the bainitic ferrite plates, there is a possibility of improving simultaneously the strength and toughness, while keeping sufficient ductility for forming and exhibiting a high resistance to damage. The high flow stresses are due to the absence of proeutectoid ferrite contrary to

existing TRIP (transformation induced plasticity) steels and to the small thickness of the bainitic ferrite laths. The TRIP effect expected from the residual austenite and the presence of islands of martensite lead to high instantaneous hardening rates. The in-use properties, such as toughness, resistance to damage, fatigue, sensibility to cut-edge and weldability are also noteworthy. In this sense, the aim of this work is the design, using phase transformation theory, of a series of carbide free bainitic steels with improved properties of strength and ductility for their application as safety parts in the automotive industries.

### 1.1 Theoretical and Thermodynamic Modeling in Steels

The bainite transformation progresses by the diffusionless growth of tiny platelets known as "sub-units" [4]. The excess carbon in these platelets partitions into the residual austenite soon after the growth event. Diffusionless growth of this kind can only occur if the carbon concentration of the residual austenite is below that given by the  $T_o$  curve. The  $T_o$  curve is the locus of all points, on a temperature versus carbon concentration plot, where austenite and ferrite of the same chemical composition have the same free energy [5]. The  $T'_o$  curve is defined similarly but takes into account the stored energy of the bainitic ferrite due to the displacive mechanism of transformation.

It follows that the maximum amount of bainite that can be obtained at any temperature is limited by the fact that the carbon content of the residual austenite must not exceed the  $T'_o$  curve of the phase diagram. Assuming that no other reaction interacts with the

bainitic ferrite formation, there are two main methods of increasing the maximum permitted amount of transformation to bainitic ferrite: by adjusting the  $T'_o$  curve to greater carbon concentrations with the use of substitutional solutes and by controlling the mean carbon concentration [6,7].

Apart from controlling the  $T'_o$  curve, substitutional solutes also affect hardenability, which is an important design parameter to avoid transformations such as proeutectoid ferrite and pearlite. For this purpose, thermodynamic and kinetics models developed to calculate the isothermal and continuous transformation diagrams, from the knowledge of the steel chemical composition, were used [8-12]. There are other design parameters such as the bainite, Widmanstätten and martensite start temperatures [5, 13].

## 1.2 Earlier Approaches in the Development of Carbide Free Bainitic Steels

The thermomechanical control processed bainitic steels have not been as successful as those quenched and tempered, because the presence of coarse cementite particles in the bainitic microstructure. The addition of ~2 wt-% silicon enables the production of a distinctive microstructure consisting of a mixture of bainitic ferrite, carbon-enriched retained austenite and some martensite. The silicon suppresses the precipitation of brittle cementite during bainite formation, and hence should lead to an improvement in toughness. The essential principles governing the optimisation of such microstructures are well established, particularly that an increase in the amount of bainitic ferrite in the

microstructure is needed in order to consume large regions of untransformed austenite, which under stress transform to hard, brittle martensite.

In previous research carried out by Bhadeshia and Edmonds [6,7] and Miihkinen and Edmonds [14-16], it was found that carbide-free bainite is in principle an ideal microstructure from many points of view. In particular, the steel has a high resistance to cleavage fracture and void formation due to the absence of carbides. There is a possibility of simultaneously improving the strength and toughness because of the ultrafine grain size of the bainitic ferrite plates, and of further enhancing the toughness by a transformation-induced plasticity effect. These original experiments [6,7] were carried out in order to demonstrate the role of the  $T_0'$  curve in greatly influencing the mechanical properties of carbide-free bainitic steels. The experimental alloys developed for this purpose are not necessarily the optimum alloys from the point of view of mechanical properties and product development.

More recently, it was demonstrated experimentally that models based on phase transformation theory can be successfully applied to the design of hot-forged carbide free bainitic steels [1,2]. In this previous work, steels alloyed with Ni were designed to achieve the highest combination of strength and toughness for bainitic microstructures after air-cooling. Toughness values of  $\sim 130 \text{ MPa m}^{1/2}$  were obtained for strength in the range of 1600-1700 MPa.

Based on these former experiences, the aim of this work is to design hot-rolled steels with the same bainitic transformation, but avoiding or reducing Ni additions for economical reasons.

## 2. Method

Designed alloys in this work were manufactured in a 60 kg vacuum induction furnace under inert atmosphere. The generator power was 80 kW. Pure (>99.9%) electrolytic iron and addition of the alloying elements one after each other were used. Carbon deoxidation was performed and an analysis of C, S, N, O was made on line during elaboration for the final adjustment of composition. Samples were hot rolled from 40 to 12 mm in several passes finishing at temperatures ranging from 900 to 930°C. The desired bainitic microstructure was obtained in all the steels by air cooling from different temperatures after an initial accelerating cooling.

Specimens for metallographic characterisation were ground and polished using standard techniques and etched in 2% nital solution for subsequent examination using light optical microscopy (LOM) and a Field Emission Gun Scanning Electron Microscope (FEG-SEM) JEOL JSM-6500F operating at 7 kV. The volume fraction of bainite was estimated by a systematic manual point-counting procedure on scanning electron micrographs.

Quantitative X-ray diffraction analysis was used to determine the fraction of retained austenite. After grinding and final polishing using 1  $\mu\text{m}$  diamond paste, the samples were etched to obtain an undeformed surface. They were then step-scanned in a SIEMENS D 5000 X-ray diffractometer using unfiltered  $\text{Cu K}\alpha$  radiation. The scanning speed ( $2\theta$ ) was less than 0.3 degree/min. The machine was operated at 40 kV and 30 mA. Retained austenite carbon content was calculated by using the lattice parameters obtained from the (200), (220) and (311) diffraction peaks.

Specimens for transmission electron microscopy (TEM) were machined down from 3 mm diameter rods. The rods were sliced into 400 mm thick discs and subsequently ground down to foils of 50 mm thickness on wet 1200 grit silicon carbide paper. These foils were finally electropolished at room temperature until perforation occurred, using a twin-jet electropolisher set at a voltage of 40 V. The electrolyte consisted of 5% perchloric acid, 15% glycerol and 80% methanol. The foils were examined in a JEOL JEM 2010 transmission electron microscope at an operating voltage of 200kV.

Tensile specimens with a section of 3 mm diameter and a gauge length of 19 mm were tested at room temperature using a Microtest EM2/100/FR testing machine fitted with a 100 kN load cell. A deformation rate of  $6 \times 10^{-4} \text{ s}^{-1}$  was used in all the experiments.

### **3. Results and Discussion**



### 3.1 Design of Advanced Bainitic Steels

As mentioned above, two steels alloyed with Ni, named Ni1 and Ni2 in Table 1, were designed in earlier work [1,2] to achieve the highest combination of strength and toughness for bainitic microstructures after hot-forging and air-cooling. Based on this first successful experience, a second set of alloys was designed to have the same bainitic transformation region in the TTT diagram and the same  $T'_o$  curve as those of Ni2 bainitic steel [1,2], but avoiding or reducing Ni additions for economical reasons. Moreover, the hardenability of the steel must be high enough to avoid the formation of proeutectoid ferrite during cooling. The chemical composition of the new designed steels (0.3BAIN 1-4) is given in Table 1. Figure 1 shows calculated  $T'_o$  curves and TTT diagrams of the designed steels in comparison with those for Ni2 steel. The  $T'_o$  curve of the different steels matches perfectly (Fig. 1(a)). Moreover, TTT diagrams in Fig. 1(b) show that all the new alloys have similar diffusionless curves and  $B_s$  and  $M_s$  temperatures, but different diffusional noses. This is not surprising since those steels have been designed to have the same maximum volume fraction of bainite at a given temperature. The calculated TTT diagrams suggested that a two-step cooling schedule was the most promising processing route to obtain a full bainitic microstructure in the new alloys.

The proposed alloys were hot rolled in several passes finishing at 930°C. The bainitic microstructure was obtained in all the steels by air cooling from different temperatures after an initial accelerating cooling at 70°C/s. Experimental data on the microstructure

are presented in Table 2. Some examples of scanning and transmission electron (SEM and TEM) micrographs of fully carbide-free bainitic microstructures (more than 75% of bainitic ferrite) in the four designed steels are shown in Figure 2. Microstructural characterisation revealed that the 0.3BAIN 1-4 alloys after air cooling from every temperature tested have the desired microstructure consisting of carbide-free upper bainite. Due to the high volume fraction of bainitic ferrite in those samples, retained austenite is mainly present as films between the subunits of bainitic ferrite. Both phases are free of carbides, as the TEM micrographs confirmed. The corresponding mechanical properties are reported in Table 3. The values presented are the average of 3 tests.

### 3.2 Adjustment on the Alloy Design to Improve in-Use Properties

Since the designed alloys have to be a reasonable solution from a final customer point of view, in-use properties such as weldability is an important issue in the alloy design procedure. Special adjustments of the chemical composition of the designed alloys are required to improve these properties. Particularly, a reduction on the carbon equivalent value is preferably. Former thermodynamic and kinetic calculations performed for the design of bainitic steels with a carbon content of 0.3 wt-% are also useful on the development of weldable bainitic steels since the influence of the average carbon content is widely known on the progress of bainite formation.

The  $T'_o$  curve is a manifestation of the formation of bainitic ferrite with full supersaturation of carbon followed by carbon partitioning between bainitic ferrite and

austenite. Steels with different carbon content will exhibit the same  $T'_o$  curve [4,17].

The driving force for the formation of new plates decreases as the carbon concentration in the untransformed austenite approaches the  $T'_o$  composition at which the free energy of ferrite and austenite phases of the same composition become identical. Carbon increases the strength of the parent austenite from which bainite grows, but nowadays it is clear that the plastic resistance of austenite is not responsible for the incomplete transformation, although some approaches have been done to considering plastic deformation as an additional source of Gibbs energy dissipation during bainite transformation [18]. Beside the independence of the  $T'_o$  curve with the average carbon content of the steel, the maximum volume fraction of bainite formed at a given transformation temperature will increase as carbon content of the steel is decreased since the critical carbon concentration for displacive transformation is reached at a later stage [6,7]. Moreover, bainite region in the TTT diagram is expected to be shifted to higher temperatures and shorter times as carbon content is reduced. Bear in mind that carbon is a strong austenite stabilizer. From the models, 0.2BAIN 1 and 0.2BAIN 3 steels (Table 1) were proposed to improve in-use properties on former advanced bainitic steels.

The third set of alloys with a carbon content of 0.2 wt-% was manufactured as 180x80x12 mm<sup>3</sup> plates. Specimens were hot rolled in several passes finishing at 913°C for 0.2BAIN 1 and 904°C in 0.2BAIN 3. The desired bainitic microstructure was obtained in both steels by air cooling from different temperatures (500 and 550°C) after an initial accelerating cooling at ~50°C/s. Microstructure data of both steels are

presented in Table 4. As an example, Figure 3 shows SEM and TEM micrographs of the microstructure obtained after air cooling from 500°C and 550°C in 0.2BAIN 1 and 0.2BAIN 3 steels. Experimental results reveal that both steels have the desired microstructure consisting of mainly bainitic ferrite and retained austenite. Martensite was not present in the microstructure. The high volume fraction of bainitic ferrite in these samples,  $\geq 90\%$ , suggests that austenite will be homogeneously distributed in the form of thin films of austenite along plate boundaries, as SEM and TEM micrographs confirmed (Figure 3). This morphology of austenite is expected to influence favorably on the ductility [19, 20].

Finally, TEM micrographs in Figure 3 confirmed that the microstructure in both steels consists of carbide-free upper bainite. Resultant microstructures of 0.2BAIN 1 and 3 steels are very similar to those obtained in the second set of alloys with 0.3 wt-% C, except for a reasonable decrease of  $\sim 100$  HV in hardness detected in the bainitic microstructures of the lower carbon alloys.

The tensile test results of 0.2BAIN 1 and 3 steels are reported in Table 5 and represented in Figure 4 in comparison with 0.3BAIN 1-4 steels as well as other commercial steels. The values presented are averages of 3 tests. Because of the lack of material, tensile specimens with the same section (3 mm diameter) and shorter gauge length (9 mm) than those used in 0.3BAIN 1-4 steels were tested at room temperature. A deformation rate of  $6 \times 10^{-4} \text{ s}^{-1}$  was again used in all the experiments. Systematic errors in YS and TE measurements are caused by the limited gauge length of the tensile

specimens which un-enabled the use of extensometer (10 mm in base length) during testing. Thus, the YS values in Table 5 were estimated from the load-cross head displacement plot, taking the gauge length of the specimen (9 mm) as the base length. Their corresponding errors were determined by comparison of the YS values determined from load-cross head displacement plot and those YS values given using the extensometer for 0.3BAIN steels. Results demonstrated that an overestimation of about 20% on YS values might be reached. On the other hand, TE values in 0.2BAIN and 0.3BAIN steels would be comparable only if a correction based on the slimmness ratio [21] is performed in TE values reported in Table 5. Thus, the revised TE values in 0.2BAIN steels are found to be 10% lower than those reported in Table 5. Beside this correction, optimum YS and TE combination were reached reducing carbon content in the designed steels.

In general, results suggest that 0.2BAIN 1 and 3 steels have a considerable potential for automotive application since they can reach very high tensile strength, above 1300 MPa while keeping a significant ductility. Their total elongations are comparable to those in TRIP steels, very impressive for such high YS and UTS. Regarding the products  $UTS \times TE$  reached by these steels (higher than 30,000 MPa%), the properties are higher than the ferritic TRIP steels under developments (typically 22,500 MPa%) [22]. In terms of formability, additional investigations should be performed. However, the present results suggest that the ratio YS/UTS is low as those obtained in DP steels (polygonal ferrite and martensite as hard phase) which can be beneficial for drawability. Likewise, the poor stretch flangeability of TRIP assisted steels may be essentially overcome by replacing the ferrite matrix with bainitic ferrite matrix since the bainitic

steel generally possesses an excellent stretch flangeability due to their uniform fine lath structure [23]. Regarding bendability, a homogenous microstructure as that reached in bainitic steels is also desirable [24].

### 3.3 Role of Microstructural Features on Mechanical Properties

The main microstructural contribution to the strength of bainite is from the extremely fine grain size of bainitic ferrite, typically 10  $\mu\text{m}$  long and  $\sim 0.2 \mu\text{m}$  thick (see TEM micrographs in Figures 2 and 3). This morphology gives small mean free path for dislocation glide. On the contrary, it is difficult to separate the effect of retained austenite on strength in these steels from other factors. Qualitatively, austenite can affect the strength in several ways; residual austenite can transform to martensite during cooling to room temperature, thus increasing the strength (see the results for the steel 0.3BAIN 1 after air cooling from 450  $^{\circ}\text{C}$ ). On the other hand, retained austenite can further increase the strength by transforming to martensite during testing, similar to the behavior of TRIP steels.

In addition, tensile elongation is controlled by the volume fraction of retained austenite. Retained austenite is a ductile phase compared to the bainitic ferrite and would be expected to enhance ductility. The resultant retained austenite volume fraction in the majority of the samples is about 10%, minimum amount of austenite required to reach an acceptable ductility [19]. Bhadeshia [19] demonstrated that the formation of strain-induced martensite can only be tolerated if the austenite maintains a uniform and percolated structure through the material. In this sense, the very low initial retained

austenite content (3%) could explain the slightly poorer ductility exhibited in 0.3BAIN 4 / 500 ° C sample.

Beside the amount of retained austenite, morphology is also an important factor to be considered on the mechanical stability of austenite. It is necessary to distinguish between the blocky morphology of austenite located between the sheaves of bainite and the films of austenite which are retained between the subunits within a given sheaf of bainite. Retained austenite would be expected to enhance ductility as far as the austenite is homogeneously distributed along plate boundaries (film austenite). However, isolated pools of austenite (blocky austenite) would influence unfavorably on both elongation and UTS. As mentioned above, SEM and TEM micrographs in Figures 2 and 3 revealed that austenite is mainly homogeneously distributed in the form of thin films of austenite along plate boundaries in all the designed steels. This fact will explain the similarity on ductility values among the designed steels.

#### **4. Conclusions**

A design procedure based on theory alone has been used to design the alloy composition and suitable control processing of hot rolled advanced bainitic steels. The designed steels, with a microstructure consisting of a mixture of bainitic ferrite and retained austenite, have achieved the highest strength and toughness combination to date for bainitic steels in as hot rolled conditions. On the basis of these preliminary results, the tough bainitic ferrite matrix and the heterogeneities in phases' hardness for

carbide free bainitic steels might be a solution to the lack of stretch flangeability and bendability of ultra high strength steel sheets such as dual phase steels and TRIP steels.

## **Acknowledgements**

The authors gratefully acknowledge the support of Spanish Ministerio de Ciencia y Tecnología Plan Nacional de I+D+I (2004-2007) funding this research under the contract MAT2007 – 63873. All of us want to thank to T. Iung and S. Allain (ARCELOR RESEARCH) for manufacturing the designed alloys.

## **References**

- [1] Caballero FG, Bhadeshia HKDH, Mawella KJA, Jones DG, Brown P. Design of novel high strength bainitic steels: Part 1. Mater Sci Technol 2001;17:512-6.
- [2] Caballero FG, Bhadeshia HKDH, Mawella KJA, Jones DG, Brown P. Design of novel high strength bainitic steels: Part 2. Mater Sci Technol 2001;17:517-22.
- [3] Caballero FG, Santofimia MJ, Capdevila C, García-Mateo C, García de Andrés C. Design of advanced bainitic steels by optimization of TTT diagrams and  $T_0$  curves. ISIJ Int 2006;46:1479-88.
- [4] Bhadeshia HKDH, Edmonds DV. The mechanism of bainite formation in steels. Acta Metall 1980;28:1265-73.
- [5] Bhadeshia HKDH. A rationalisation of shear transformations in steels. Acta Metall 1981;29:1117-30.



- [6] Bhadeshia HKDH, Edmonds DV. Bainite in silicon steels: new composition-property approach. Part I. *Met Sci* 1983;17:411-9.
- [7] Bhadeshia HKDH, Edmonds DV. Bainite in silicon steels: new composition-property approach. Part II. *Met Sci* 1983;17:420-5.
- [8] Materials Algorithms Project (MAP), Department of Materials Science and Metallurgy, University of Cambridge, U. K.: <http://www.msm.cam.ac.uk/map>.
- [9] Bhadeshia HKDH. A thermodynamic analysis of isothermal transformation diagrams. *Met Sci* 1982;16:159-65.
- [10] Jones SJ, Bhadeshia HKDH. Kinetics of the simultaneous decomposition of austenite into several transformation products. *Acta Metall* 1997;45:2911-20.
- [11] Parker SV. Modelling of Phase Transformation in Hot Rolled Steels. PhD Thesis, University of Cambridge, U. K.; 1997.
- [12] Caballero FG, Capdevila C, García de Andrés C. Evaluation and review of the simultaneous transformation model in high strength low alloy steels. *Mat Sci Technol* 2002 ;18:534-40.
- [13] García-Mateo C, Bhadeshia HKDH. Nucleation theory for high carbon bainite. *Mat Sci Eng* 2004;378A:289-92.
- [14] Miihkinen VTT, Edmonds DV. Microstructural examination of two experimental high-strength bainite low-alloy steel containing silicon. *Mater Sci Technol* 1987;3:422-31.
- [15] Miihkinen VTT, Edmonds DV. Tensile deformation of two experimental high-strength bainite low-alloy steel containing silicon. *Mater Sci Technol* 1987;3:432-40.
- [16] Miihkinen VTT, Edmonds DV. Fracture toughness of two experimental high-strength bainite low-alloy steel containing silicon. *Mater Sci Technol* 1987;3:441-9

- [17] Zener C. Kinetics of the Decomposition of Austenite. Trans AIME 1946;167:550-95.
- [18] Quidort D, Bouaziz O, Brechet Y. The role of carbon on the kinetics of bainite transformation in steels. In: Buddy Damm E, Merwin MJ, editors. Austenite Formation and Decomposition; Warendale, PA, 2003, p. 15-25
- [19] Bhadeshia HKDH. Bessemer Memorial Lecture: The dimensions of steel. Ironmaking and Steelmaking 2007;34:194-199.
- [20] Garcia-Mateo C, Caballero FG. The role of retained austenite on mechanical properties of novel bainitic microstructures. Mater Trans 2005;46:1839-46.
- [21] Holt JM. Uniaxial tension testing. In: ASM International Handbook. Mechanical testing and evaluation. Materials Park, Ohio, 2000, 124-42.
- [22] Jacques P, Petein A, Harlet P. Improvement of mechanical properties through concurrent deformation and transformation. In: Int.Conf. onTRIP-aided high strength ferrous alloys. Ghent, Belgium, 2002, p. 281-85.
- [23] Sugimoto K, Nakano K, Song S, Kashima T. Retained austenite characteristics and stretch-flangeability of high-strength low-alloy TRIP type bainitic sheet steels. ISIJ Int 2002;42:450-55.
- [24] Takahashi M. Nippon Steel Tech. Rep. No 88, 2003.

## Figure Captions

Fig. 1. (a)  $T'_o$  curve and (b) TTT diagram of the designed steels.

Fig. 2. SEM and TEM micrographs of the second set of designed steels after air cooling from different temperatures: (a, b) 0.3BAIN 1 / 600°C, (c, d) 0.3BAIN 2 / 500°C, (e, f) 0.3BAIN 3 / 500°C, (g, h) 0.3BAIN 4 / 500°C.

Fig. 3. SEM and TEM micrographs of the third set of designed steels after air cooling from different temperatures: (a, b) 0.2BAIN 1 / 500°C, (c, d) 0.2BAIN 1 / 550°C, (e, f) 0.2BAIN 3 / 500°C, (g, h) 0.2BAIN 3 / 550°C.

Fig. 4. Yield strength and total elongation of advanced bainitic steels in comparison with other commercial steels.

ACCEPTED MANUSCRIPT

## Tables

Table 1

Actual chemical composition of designed advanced bainitic steels (wt-%).

Steel	C	Si	Mn	Ni	Cr	Mo	V
First set of alloys:							
Ni1	0.31	1.51	<0.01	3.52	1.44	0.25	0.10
Ni2	0.30	1.51	<0.01	3.53	1.42	0.25	---
Second set of alloys:							
0.3BAIN 1	0.29	1.50	2.25	---	---	0.26	---
0.3BAIN 2	0.29	1.46	1.97	---	0.46	0.25	---
0.3BAIN 3	0.29	1.49	1.56	---	1.47	0.25	---
0.3BAIN 4	0.27	1.71	1.53	1.47	0.17	0.24	---
Third set of alloys:							
0.2BAIN 1	0.22	1.50	2.23	---	---	0.25	---
0.2BAIN 3	0.21	1.46	1.56	---	1.49	0.24	---

Table 2

Quantitative data on microstructure of the second set of designed steels. FCT is interrupted accelerating cooling temperature;  $V_b$  is the volume fraction of bainitic ferrite;  $V_M$  is the volume fraction of martensite;  $V_\gamma$  is the volume fraction of austenite;  $x_\gamma$  is the carbon content in austenite.

Steel / FCT	$V_b$	$V_M$	$V_\gamma$	$x_\gamma$ (wt.%)
0.3BAIN 1 / 450°C	$0.73 \pm 0.04$	$0.24 \pm 0.05$	$0.03 \pm 0.01$	$0.66 \pm 0.06$
0.3BAIN 1 / 600°C	$0.76 \pm 0.03$	$0.21 \pm 0.04$	$0.03 \pm 0.01$	$0.95 \pm 0.01$
0.3BAIN 2 / 500°C	$0.77 \pm 0.04$	$0.13 \pm 0.05$	$0.10 \pm 0.01$	$1.14 \pm 0.03$
0.3BAIN 2 / 550°C	$0.80 \pm 0.04$	$0.09 \pm 0.05$	$0.10 \pm 0.01$	$1.26 \pm 0.07$
0.3BAIN 3 / 500°C	$0.88 \pm 0.02$	$0.02 \pm 0.03$	$0.11 \pm 0.01$	$1.03 \pm 0.05$
0.3BAIN 3 / 550°C	$0.86 \pm 0.02$	$0.03 \pm 0.04$	$0.11 \pm 0.01$	$1.04 \pm 0.04$
0.3BAIN 4 / 500°C	$0.88 \pm 0.02$	$0.09 \pm 0.04$	$0.03 \pm 0.01$	$1.26 \pm 0.07$

Table 3

Tensile properties results at 20°C of the second set of designed steels. FCT is interrupted accelerating cooling temperature; YS yield strength; UTS ultimate tensile strength; TE total elongation.

Steel/ FCT	YS (MPa)	UTS (MPa)	TE (%)
0.3BAIN 1 / 450°C	1240 ± 31	1796 ± 21	18 ± 1
0.3BAIN 1 / 600°C	1204 ± 29	1701 ± 9	16 ± 1
0.3BAIN 2 / 500°C	1187 ± 16	1606 ± 30	17 ± 2
0.3BAIN 2 / 550°C	1128 ± 32	1539 ± 21	16 ± 2
0.3BAIN 3 / 500°C	1194 ± 35	1652 ± 6	18 ± 1
0.3BAIN 3 / 550°C	1204 ± 18	1642 ± 12	18 ± 1
0.3BAIN 4 / 500°C	1339 ± 16	1763 ± 18	16 ± 1

Table 4

Quantitative data on microstructure of the third set of designed steels. FCT is interrupted accelerating cooling temperature;  $V_b$  is the volume fraction of bainitic ferrite;  $V_M$  is the volume fraction of martensite;  $V_\gamma$  is the volume fraction of austenite; and  $x_\gamma$  is the carbon content in austenite.

Steel / FCT	$V_b$	$V_M$	$V_\gamma$	$x_\gamma$ (wt-%)
0.2BAIN 1 / 500°C	$0.91 \pm 0.02$	---	$0.09 \pm 0.01$	$1.26 \pm 0.06$
0.2BAIN 1 / 550°C	$0.93 \pm 0.02$	---	$0.09 \pm 0.01$	$1.15 \pm 0.03$
0.2BAIN 3 / 500°C	$0.90 \pm 0.02$	---	$0.11 \pm 0.01$	$1.04 \pm 0.07$
0.2BAIN 3 / 550°C	$0.91 \pm 0.02$	---	$0.12 \pm 0.01$	$1.02 \pm 0.06$

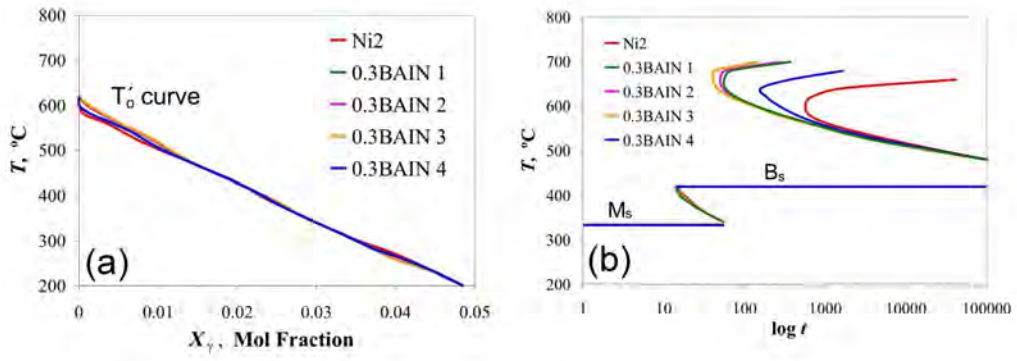
Table 5

Tensile properties results at 20°C of the third set of designed steels. FCT is interrupted accelerating cooling temperature; YS yield strength; UTS ultimate tensile strength; TE total elongation.

Steel/ FCT	YS (MPa)	UTS (MPa)	TE (%)
0.2BAIN 1 / 500°C	1192 ± 82	1382 ± 31	24 ± 2
0.2BAIN 1 / 550°C	1146 ± 17	1347 ± 8	25 ± 3
0.2BAIN 3 / 500°C	1033 ± 64	1319 ± 12	23 ± 2
0.2BAIN 3 / 550°C	999 ± 54	1306 ± 16	25 ± 3

ACCEPTED MANUSCRIPT

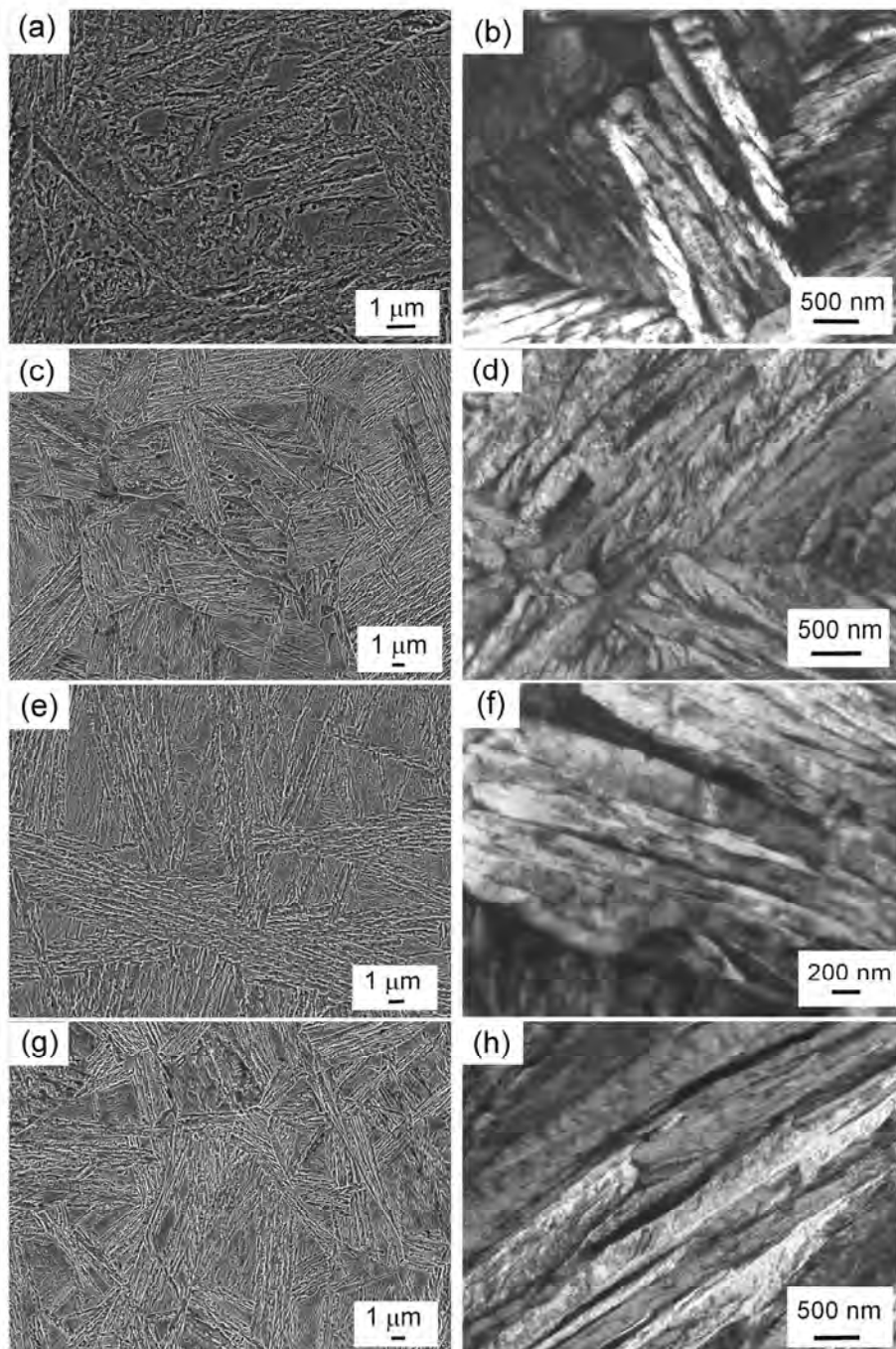




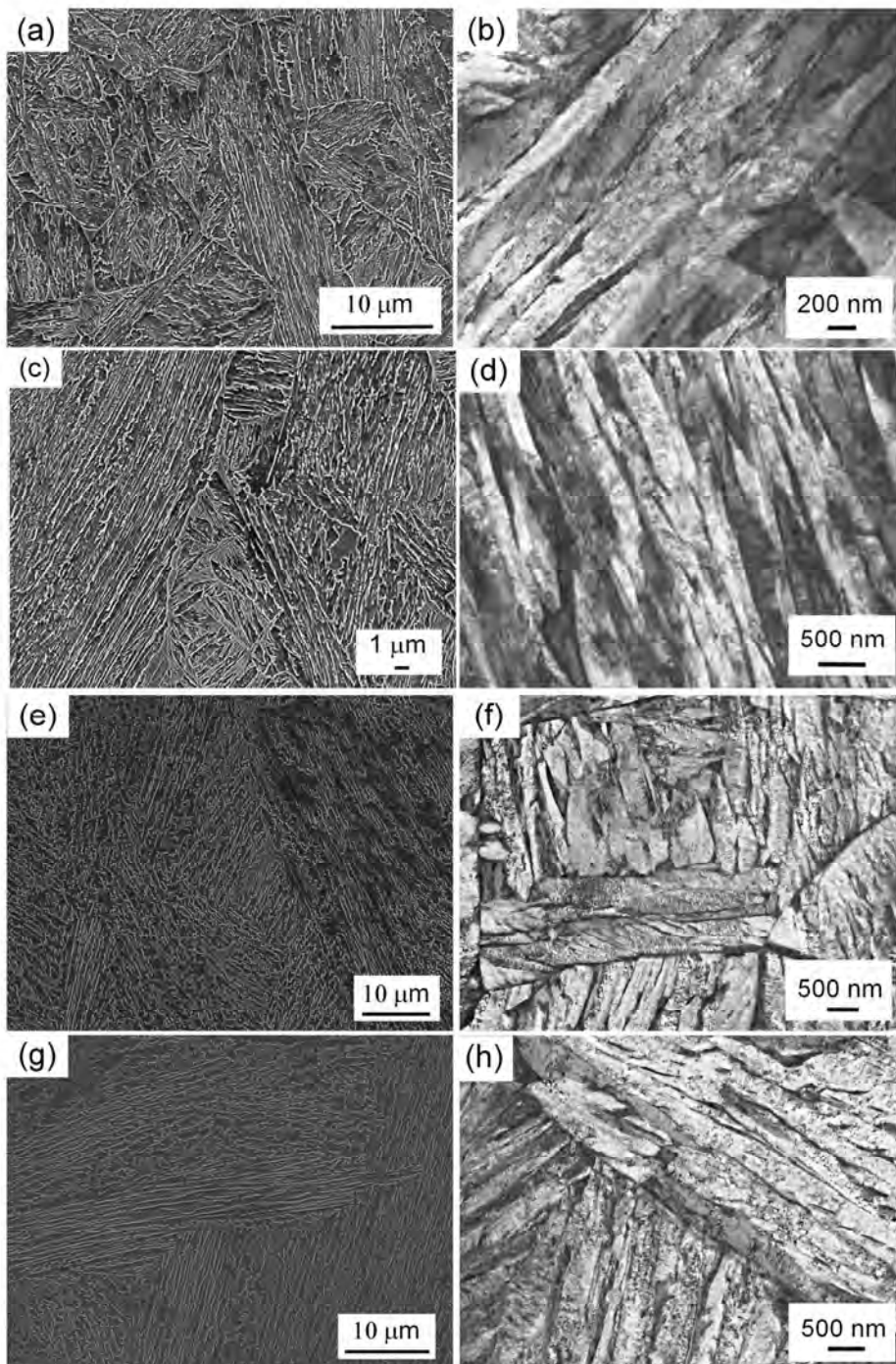
**Fig.1**

ACCEPTED MANUSCRIPT

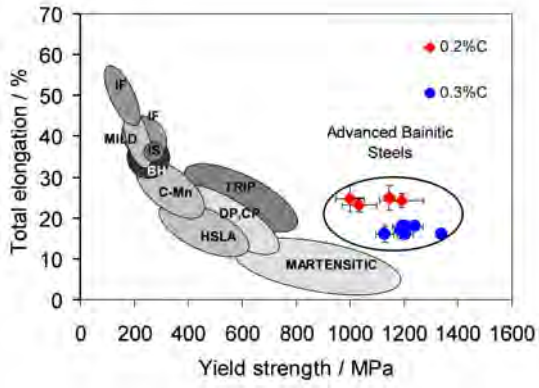
**Fig.2**



**Fig.3**



**Fig.4**



ACCEPTED MANUSCRIPT